

In-vitro pliability assessment of embolization coils for intracranial aneurysm treatment

Rui Zhao^a, Jianmin Liu^a, Steven McComas^b, Jenny Guo^b, Gaurav Girdhar^{b,*}

^a Department of Neurosurgery, Changhai Hospital, Shanghai 200433, China

^b Medtronic PLC, 9775 Toledo Way, Irvine, CA 92618, United States

ARTICLE INFO

Keywords:

Coiling
Softness
Pliability
Force
Aneurysm
Rupture

ABSTRACT

Background: Embolization coils have routinely been used to treat intracranial aneurysms via an endovascular approach. Soft coils are typically viewed as the best design for filling and finishing the aneurysms to achieve a higher packing density and are hypothesized to exert a lower force against the aneurysm wall during deployment. We report here an in vitro pliability test method to assess clinically relevant coil softness and compare these metrics for two commercially available framing and finishing coil products.

Methods: A force measurement sensor was affixed onto a side-wall synthetic aneurysm model to continuously measure forces on the aneurysm wall during coil deployment at a fixed delivery rate. A quantitative overall energy metric (average work number or AWN) was calculated from the force-displacement graph representing coil delivery into the aneurysm. Two groups of coils were evaluated: (a) finish coil group ($N = 20$ ea.): Axiom™ Prime Extra Soft coil (ES) and Target™ 360 Nano coil (Nano), and (b) frame coil group ($N = 20$ ea.): Axiom™ Prime FC coil (FC) and Target™ 360 Standard coil (Standard).

Results: (a) In the finish coil group, AWN was measured as: ES (0.53 ± 0.09 gf-cm) and Nano (0.99 ± 0.21 gf-cm). (b) In the frame coil group, AWN was measured as FC (2.54 ± 0.53 gf-cm) and Standard (4.48 ± 0.52 gf-cm). In both groups, Axiom Prime coils had statistically lower measures of AWN and therefore higher pliability compared to Target coils ($p < .001$).

Conclusions: The in-vitro pliability test method offers quantitative metrics to assess coil softness during deployment in a clinically relevant aneurysm model.

1. Introduction

Endovascular coiling has been widely used for treatment of intracranial aneurysms. Platinum coils are typically deployed until a packing density sufficient to cause occlusion of the aneurysm sac [3]. A typical medium to large intracranial aneurysm coiling procedure uses framing (stable), filling (soft) and finishing (extra soft) coils – in that order. One of the worst risks associated with endovascular coiling is intraprocedure aneurysm rupture (IAR) [2,5,9]. Although the IAR occurrence is low (1–8%), it markedly increases the risk of morbidity and mortality [9]. This has been broadly correlated to aneurysm size [12] and certain aneurysm locations [9] that are associated with a higher perforation risk during intervention with guidewires, microcatheters and coils [6]. There is also a limited IAR dependence on coil placement sequence as well as microcatheter placement and tracking. For instance, in some cases IAR occurrence has been reported during placement of the first coil [6] (usually a framing coil) or during subsequent coils [15] (in

some instances this could be attributed to overpacking). IAR is also seen both with soft coils [7] in addition to framing coils [5]. From histological post-mortem evaluations, the average wall thickness of an intracranial aneurysm is approximately $50 \mu\text{m}$ [1]. The intracranial aneurysm wall structure is heterogeneous and the thickness has been shown to be inversely correlated to localized wall shear stress (and thereby rupture risk) [4,13]. Therefore, the localized force exerted on the aneurysm wall during interventions should be minimized. Proper coil selection in addition to the rate of deployment of coils (with visual feedback) could be one of the factors for minimizing IAR risk.

Previous reports have quantified the average force on the aneurysm wall during coil deployment in an in vitro setting [10,11]. These reports show the stiffness differences that are apparent between framing and filling coils and also show a correlation between distal force exerted on the aneurysm wall and the proximal push force used to deliver the coil [10]. A limitation in these measurements was either the use of a straight vessel anatomy leading up to the aneurysm [10] or the measurement of

* Corresponding author at: Medtronic PLC, 9775 Toledo Way, Irvine, CA 92618, United States

E-mail address: gaurav.girdhar@medtronic.com (G. Girdhar).

<https://doi.org/10.1016/j.jns.2019.116432>

Received 30 May 2019; Received in revised form 20 August 2019; Accepted 21 August 2019

Available online 22 August 2019

0022-510X/ © 2019 The Authors. Published by Elsevier B.V. This is an open access article under the CC BY-NC-ND license (<http://creativecommons.org/licenses/by-nc-nd/4.0/>).

only the proximal push force to deliver the coil [11]. Coil stiffness surrogates such as first principles calculation using Hookean assumptions [16] or a measure of final packing density of the coils in the aneurysm [14], have also been proposed. These latter methods, however, may be limited in not being able to demonstrate the higher order effects associated with coil structure and deployment in a physiological aneurysm model.

We report here a clinically relevant *in vitro* method to measure coil softness (“pliability”) and compare two commercial products – both in the framing and finishing coils categories. The two finishing coils evaluated were Axiu™ Prime ES coil (Medtronic, Irvine, CA) and Target™ 360 Nano coil (Stryker, Fremont, CA). The Prime ES coil was designed for smooth transitions within the aneurysm and this is facilitated with a smaller wire diameter, larger primary outer diameter and thinner stretch resistant strand diameter. The Target™ 360 Nano coil (Stryker, Fremont, CA) has a flexible primary wire to reduce the coil stiffness and is therefore often recommended as a finishing coil. The two framing coils evaluated were Axiu™ Prime FC coil (Medtronic, Irvine, CA) and Target™ 360 Standard coil (Stryker, Fremont, CA). The Prime FC coil consists of a complex shape that is made of 6 tangent 3/4-full loops which provide sufficient shape retention while maintaining an open loop design. The Target 360 Standard coil has a 3D shape which – according to the manufacturer – provides concentric alignment in an aneurysm with an open center for additional filling.

We utilize an energy based metric (area of the force-displacement curve; reported as “average work number or AWN”) to quantify the differences between the coils in each category. This metric represents a product of the measured components of force perpendicular to the aneurysm neck (near the top of the aneurysm dome), and the length of coil delivered (for a single coil).

2. Materials and methods

2.1. Coils

Two commercially available coils in framing and finishing segments were compared – (a) Finish coil group: Axiu™ Prime ES coil (2.5 mm × 4 cm, Medtronic, $N = 20$) and Target™ 360 Nano coil (2.5 mm × 4 cm, Stryker, $N = 20$) were delivered into the aneurysm model and force-displacement data was measured. Each coil was 2.5 mm (coil loop OD) × 4 cm (coil length), and (b) Frame coil group: Axiu™ Prime FC coil (5 mm × 15cm, Medtronic, $N = 20$) and Target™ 360 Standard coil (5 mm × 15cm, Stryker, $N = 20$) were delivered into the aneurysm model and force-displacement data was measured. Each coil was 5 mm (coil loop OD) × 15 cm (coil length).

2.2. Coil pliability measurement experimental setup

The test setup consisted of a commercially available automated tracking and measurement system (Interventional Device Testing Equipment, Machine Solution Inc. Flagstaff, AZ). A schematic of the setup is shown in Fig. 1. Briefly, the setup consists of a computer controlled proximal motor, a leveled test surface with the simulated deployment track, a synthetic ICA (Internal Carotid Artery) model, an aneurysm model, X-Y positioning calipers, video camera, and a distal load cell affixed to the spherical aneurysm model. A 20 g distal sensor (Futek Advanced Sensor Technology Inc., Irvine, CA) was affixed onto one side of the outer surface of the aneurysm model to measure the perpendicular component of the force as a coil is being deployed. The position of the microcatheter was offset relative to the neck and fixed at the level of the neck in the aneurysm model. This was done intentionally to avoid any artifacts on the force measurement from microcatheter navigation within the aneurysm.

The distal force sensor was calibrated against known standards prior to the evaluations with the coils. For each test run, the coils were inserted manually into an 0.017 in ID Echelon microcatheter (Medtronic,

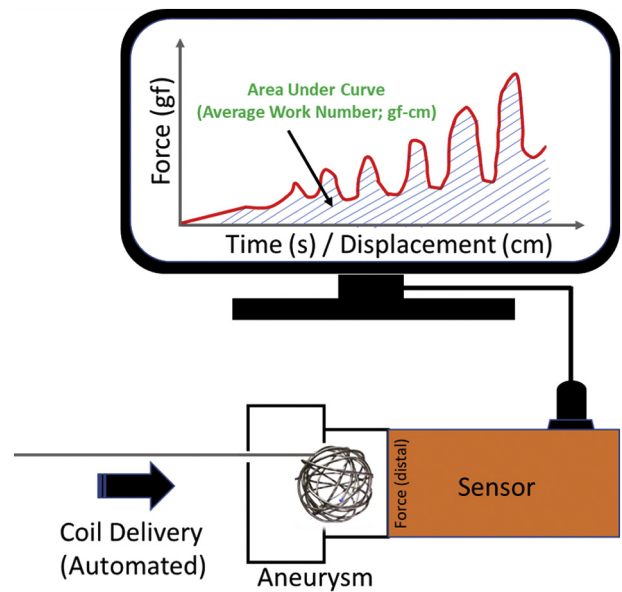


Fig. 1. Schematic of the coil pliability measurement experimental setup.

Irvine, CA) until the distal end arrived at the entrance of aneurysm model and did not advance past the neck of the aneurysm as mentioned previously. Thereafter the deployment of coils into the aneurysm was controlled with a programmable motor (no human intervention) as per pre-specified inputs. The deployment rate and total deployment length was pre-programmed as followed: (a) Finish coil group: 5 cm/min rate and 3.75 cm length, and (b) Frame coil group: 10 cm/min rate and 14 cm length. The distal force sensor recorded the perpendicular components of the force exerted by the coil against the aneurysm wall simultaneously as soon as the roller (attached to proximal motor) started to push the delivery wire. Force data was captured at a frequency of 16 Hz and combined with the video capture (visual) data for analysis later.

2.3. Force-displacement data analysis

The distal force measured for each coil during deployment against the aneurysm wall was quantified as a force-displacement curve. Peaks in the curve may be indicative of certain design characteristics of the coils - such as stiffness of coil loops, oversizing or sequential packing, and difficulty of turning or steering within the aneurysm.

We quantified and reported an averaged energy metric (Average Work Number or AWN) that can be calculated as the area under each force-displacement curve (gf-cm). Smaller AWN therefore translates to less force exerted by the coil on the wall during deployment and represents a measure of pliability of the coil.

2.4. Statistical analysis

A normality test was conducted for the AWN data. Non-normal data was transformed per Johnson's transformation prior to statistical analysis with ANOVA. Post-hoc Fishers *t*-test was conducted to identify differences between the 4 coils in the study. A significance level of 0.05 was used for all tests.

3. Results

ANOVA for AWN showed a significant difference ($p < .001$) between the coils evaluated. The results for the individual groups are described below.

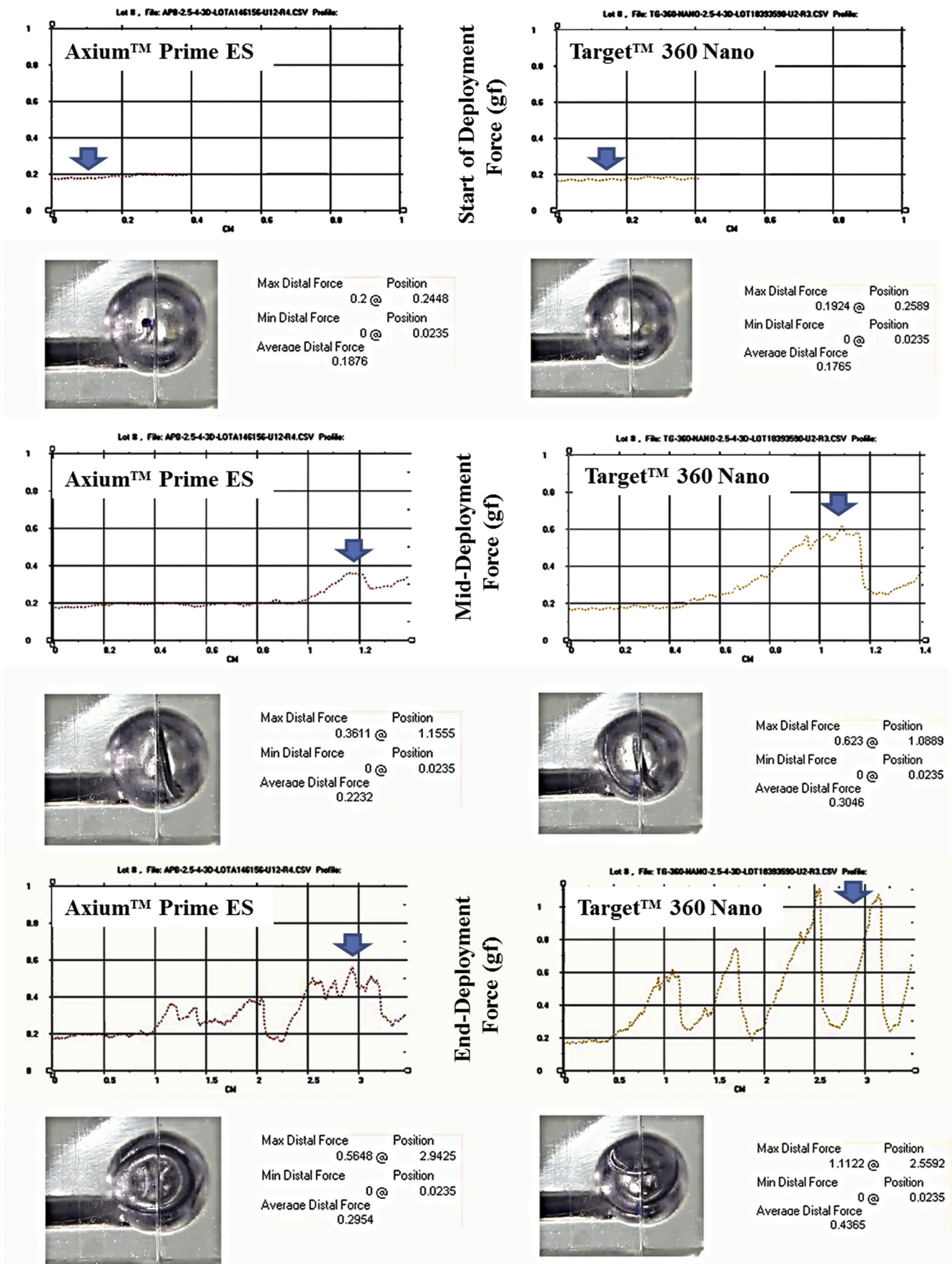


Fig. 2. Sequential deployment of the Axiom Prime ES and Target Nano coils inside the aneurysm. Force measured is shown for intial, mid-deployment and end-deployment stages, together with the corresponding video image of the coil at each stage.

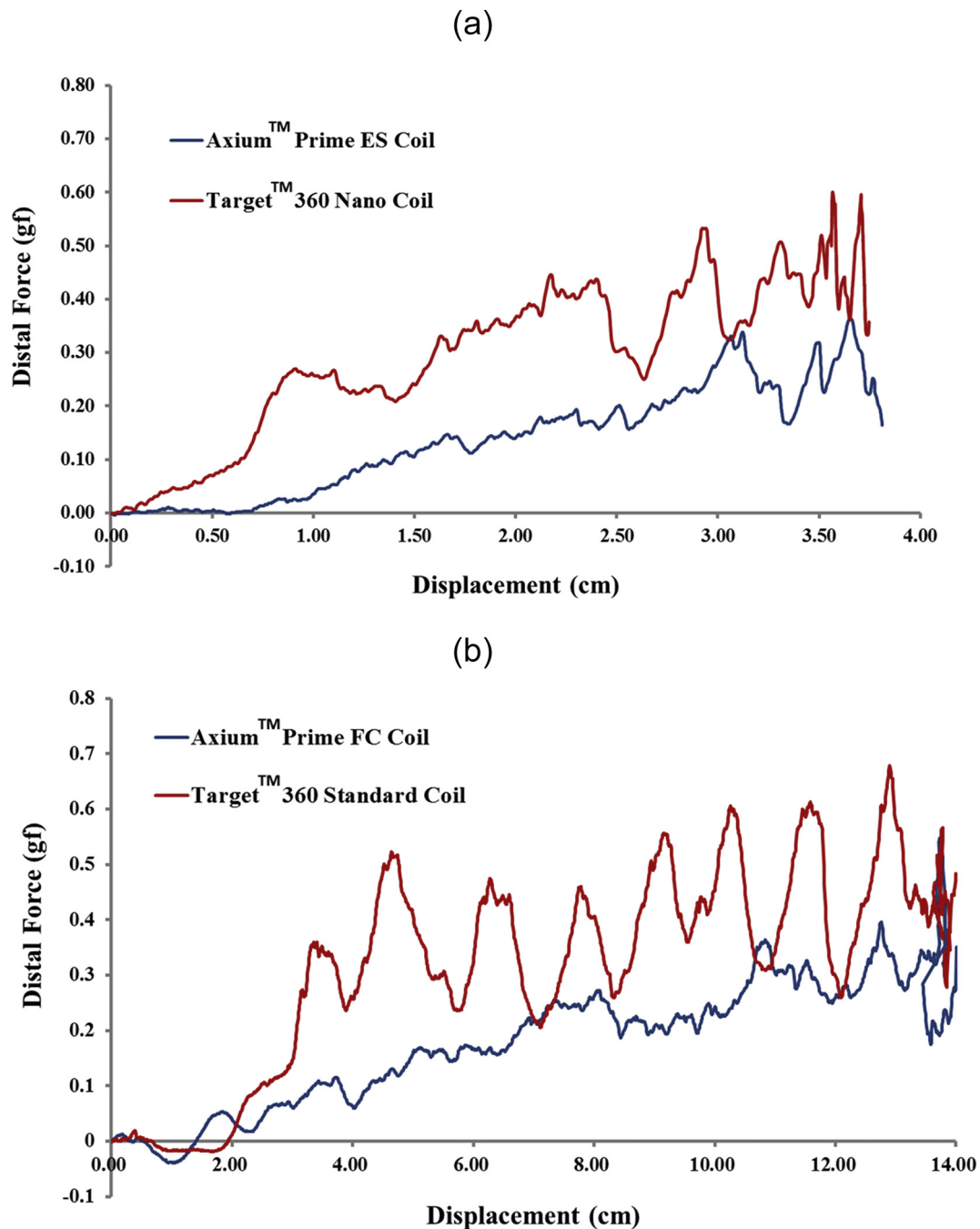


Fig. 3. (a) Measured distal force (gf) and displacement curve averaged for $N = 20$ Axium Prime ES coil and Target 360 Nano coil (b) Measured distal force (gf) and displacement curve averaged for $N = 20$ Axium Prime FC coil and Target 360 Standard coil.

3.1. Finish coil group: Axium™ Prime ES coil and Target™ 360 Nano coil

A sequential force-displacement graph showing the 3 phases (initial deployment, mid deployment and end of deployment) for a representative Axium Prime ES coil and a Target 360 Nano coil are illustrated in Fig. 2 and the Supplementary Video S1. In the beginning of deployment, the curves are flat because there is sufficient open volume in the aneurysm model and the coils were easy to deploy and bend. The peaks in the force-displacement curves are representative of the coil being pushed against the aneurysm wall. The valleys represent coil bends or loop segments and the corresponding spatial arrangement within the open space in the aneurysm. As the coil continued to fill the aneurysm model, more coil loops were formed within the progressively reduced available aneurysm volume and this translated to higher force

being detected by the distal force sensor. Thus the peaks and valleys become more apparent as a longer length of the coil is progressively deployed in the aneurysm.

The averaged ($N = 20$) force-displacement curve for each coil is shown in Fig. 3a. The AWN for the Axium™ Prime ES coil was measured as 0.53 ± 0.09 gf-cm compared with 0.99 ± 0.21 gf-cm for the Target™360 Nano coil (Fig. 4). Post-hoc Fishers *t*-test for AWN showed significant difference between the two coils ($p < .001$).

3.2. Frame coil group: Axium™ Prime FC coil and Target™ 360 Standard coil

The averaged ($N = 20$) force-displacement curve for each coil is shown in Fig. 3b. The AWN for the Axium™ Prime FC coil was measured

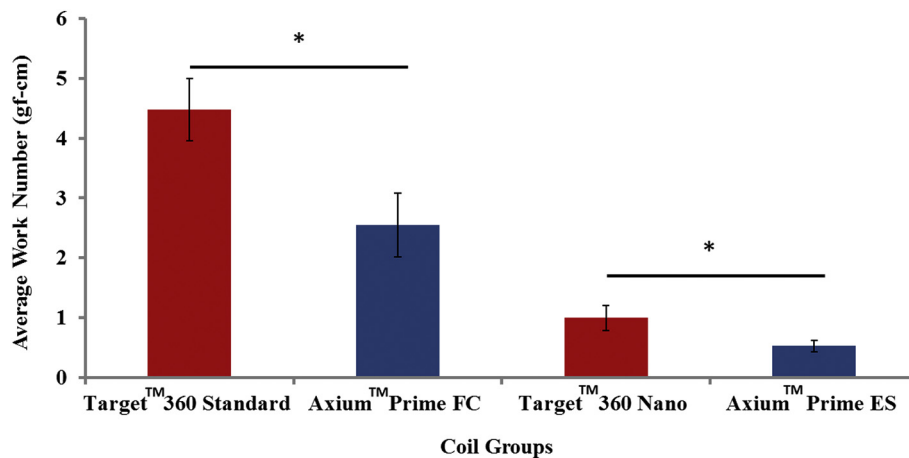


Fig. 4. Mean \pm sd (standard deviation) of Average Work Number (AWN) for Axium Prime ES and FC coils and Target 360 Standard and Nano coils.

as 2.51 ± 0.59 gf-cm compared with 4.48 ± 0.52 gf-cm for the Target™ 360 Standard coil (Fig. 4). Post-hoc Fishers *t*-test for AWN showed significant difference between the two coils ($p < .001$).

Similar peaks and valleys characteristic of coil deployment were observed in the framing coil groups (Fig. 3b). However, notable differences between the magnitude of the force gradient between the peaks and valleys were measured for the Target 360 Standard coil as opposed to the Axium Prime FC coil. The force-displacement curve overlaid with a real-time visual image of coil deployment at the same time points for the two framing coils shows characteristics similar to the Finish coil group – the force gradients (peaks and valleys) become more apparent as the coils are progressively deployed in the aneurysm.

The Target 360 Standard coil appears to offer significant resistance to rearrangement within the aneurysm sac. Conversely, the loops in the Axium Prime FC coils appear to rotate more smoothly and rearrange within the available aneurysm sac volume. With the Target 360 Standard coil, compartmentalization may occur within the aneurysm and may account for the higher magnitude of force gradients (Fig. 3b) as opposed to a stable “basket” like structure with the Prime FC coil resulting in lower force gradients.

4. Discussion

Coil softness during deployment in an aneurysm is usually a subjective feeling and can vary between interventionists. Stiffness of a coil is often defined by the spring constant of the secondary structure due to the similarity of the coil structure to a spring in appearance [16]. However, the coil is not compressed to fill the aneurysm during a clinical endovascular procedure – instead – it is often bent to fit the limited space within the aneurysm sac. It is therefore much easier to bend a coil than to compress it, and for this reason, one can hardly compress a spring without buckling it first [8]. The final coil structure and especially the coil behavior and its engagement with the aneurysm wall during deployment (higher order effects) are not considered in the simple stiffness (force constant *K*) calculation. This theoretical coil stiffness factor (*K*) can be calculated as follows [16]:

$$K = \frac{D_1^4 G}{8D_2^3 n}; \text{Stiffness} \propto \frac{D_1^4}{D_2^3}$$

where, D_1 is the coil wire diameter, G is the shear modulus of the coil wire, D_2 is primary coil outer diameter (OD), and n is the number of windings per unit distance. The theoretical coil stiffness (*K* factor) of the two coil groups is shown in Table 1. This *K* factor calculation shows that the Target coils should be theoretically stiffer than the Axium Prime coils. Our experimental analysis performed at a constant rate of deployment with the two coil groups and coil types confirms this trend

for coil stiffness: Target Standard > Axium Prime FC > Target Nano > Axium Prime ES (Fig. 4). The ease deformation of a coil within an aneurysm is multifactorial and may be influenced by the thickness of the Polypropylene (PP) filament (stretch resistant member), coil loop diameter, and secondary shape, besides others. Axium™ Prime ES coil has a smaller loop diameter (2.221 mm) compared to the Nano coil (3.634 mm) and therefore may encounter less loop compression within the aneurysm sac. Additionally, the thinner filament of the Axium Prime coils relative to the Target coils (Table 1) may result in the lower force observed (Fig. 3a and b) when the coils start to bend and rearrange within the available aneurysm volume.

Higher order effects like the secondary and tertiary structure of the coil and conformability to the aneurysm sac may also account for the offset seen between Axium Prime and Target coils in the two coil groups. For instance, the Target™ 360 Standard coil has a nominal loop OD of 5.577 mm (Table 1) and a well-known pre-determining secondary shape feature due to its closed loop design. The more each progressive coil loop is compressed during deployment, the higher the corresponding compression force is against the aneurysm wall. This may lead to stacking together of the loops within the aneurysm and cause compartmentalization (non-uniform coil loop distribution). This feature may be notable during the current evaluation as the increased resistance with progressive coil deployment is also apparent in the corresponding peaks observed in the force-displacement curve (Fig. 3b). The resistance to coil rearrangement may be less prominent with the Axium Prime FC coils presumably due to the complex shape design. This design may allow the progressive coil loops to support each other and forming a stable structure allowing less resistance during rotation and improved conformability to the aneurysm wall.

Another notable feature is the difference in peak force towards the end of the loop. This is more apparent for the Target 360 Standard coil and Nano coil as opposed to the Axium Prime FC coil and ES coil. Higher forces towards the end of deployment or aneurysm fill could potentially result in loops herniating within the parent vessel – a notable limitation requiring the use of aneurysm bridging stents to mitigate. Conversely, lower forces towards the end of deployment will allow progressive packing of the aneurysm closer to the neck – with less chances of loop herniation into the parent vessel.

The combination of tactile and visual feedback during coil embolization remains a challenge. This is because it is often difficult to discern small magnitude of forces that may potentially cause IAR. This tactile feedback remains subjective and can vastly differ between operators. Therefore, it is imperative to address these issues at the coil design stage. We have demonstrated in this manuscript the utility of an in vitro pliability test that allows investigation of coil design attributes and the specific impact on overall safety of delivery within an aneurysm that could mitigate or prevent IAR. We have also demonstrated a proof-of-

Table 1

Dimensions of the coils in Finish and Frame groups: wire diameter (D_1), primary coil (D_2), nominal loop and polypropylene (PP) filament outer diameters (OD), and corresponding K factor.

Group	Coil	Wire diameter (D_1 , inch)	Primary coil OD (D_2 , inch)	K factor (D_1^4/D_2^3) 1×10^{-6}	Nominal loop OD (mm)	PP filament OD (inch) (2 strands)
Finish coil group	Axium™ Prime ES	0.00130	0.0108	2.267	2.221	0.0011
	Target™ 360 Nano	0.00125	0.0100	2.441	3.634	0.0014
Frame coil group	Axium™ Prime FC	0.00200	0.0125	8.192	4.770	0.0014
	Target™ 360	0.00195	0.0101	13.99	5.577	0.0015
	Standard					

concept feasibility of the test method by comparing the effect of primary design features of two commercially available coils on overall coil delivery performance. The difference in AWN measurements illustrate the point that minor dimensional and structural differences may have on overall impact on coil performance and procedural safety.

We acknowledge that our method has significant limitations and departs from the clinical use of coils as follows: (a) coils were delivered at a pre-programmed constant rate into the aneurysm – clinically an operator may choose to slow down based on the visual and often less perceptible tactile feedback, (b) a rigid acrylic aneurysm model was utilized as opposed to a material with mechanical properties similar to the aneurysm wall, (c) the microcatheter was placed at the neck of the aneurysm to remove the influence of microcatheter movement on the forces being measured, (d) there was no physiological blood flow during deployment, (e) measurements were conducted at only one representative coil deployment rate, for single coils and one size of coils only, and in a single aneurysm model, and (f) only the perpendicular component of the force exerted on the aneurysm wall was measured. We note that this was all done intentionally to be able to illustrate the differences between the two coil groups and to create a controlled scenario for a 1:1 comparison between coil types in terms of forces exerted on the aneurysm wall during deployment. Investigation of the effects of aneurysm shapes and the position of the microcatheter on pliability measurement will be the subject of future research.

5. Conclusions

The in-vitro coil pliability test method quantitatively detects forces exerted on a synthetic aneurysm wall during progressive coil deployment. In a simulated synthetic aneurysm model, the Axium Prime FC and ES coils were found to exert significantly lower forces on the aneurysm wall relative to Target 360 Standard and Nano coils respectively.

Supplementary data to this article can be found online at <https://doi.org/10.1016/j.jns.2019.116432>.

References

[1] T. Abruzzo, G.G. Shengelaia, R.C. Dawson 3rd, D.S. Owens, C.M. Cawley,

- M.B. Gravanis, Histologic and morphologic comparison of experimental aneurysms with human intracranial aneurysms, *Am. J. Neuroradiol.* 19 (1998) 1309–1314.
- [2] J.M. Ahn, J.S. Oh, S.M. Yoon, J.H. Shim, H.J. Oh, H.G. Bae, Procedure-related complications during endovascular treatment of intracranial saccular aneurysms, *J. Cerebrovasc. Endovasc. Neurosurg.* 19 (2017) 162–170.
- [3] M.H. Babiker, L.F. Gonzalez, F. Albuquerque, D. Collins, A. Elvikis, D.H. Frakes, Quantitative effects of coil packing density on cerebral aneurysm fluid dynamics: an in vitro steady flow study, *Ann. Biomed. Eng.* 38 (2010) 2293–2301.
- [4] R. Blankena, R. Kleinloog, B.H. Verweij, P. van Ooij, B. Ten Haken, P.R. Luijten, et al., Thinner regions of intracranial Aneurysm Wall correlate with regions of higher wall shear stress: a 7T MRI study, *Am. J. Neuroradiol.* 37 (2016) 1310–1317.
- [5] C.H. Chang, Y.J. Jung, J.H. Kim, Intraprocedural rupture management for intracranial aneurysm rupture during coil embolization by manual common carotid artery compression, *J. Clin. Neurosci.* 22 (2019) 273–276.
- [6] A. Doerfler, I. Wanke, T. Egelhof, U. Dietrich, S. Asgari, D. Stolke, et al., Aneurysmal rupture during embolization with Guglielmi detachable coils: causes, management, and outcome, *Am. J. Neuroradiol.* 22 (2001) 1825–1832.
- [7] G. Jindal, T. Miller, M. Iyohe, R. Shivashankar, V. Prasad, D. Gandhi, Small intracranial aneurysm treatment using target® Ultrasoft™ coils, *J. Vasc. Interv. Neurol.* 9 (2016) 46–51.
- [8] L.D. Jou, Softness of endovascular coils, *Am. J. Neuroradiol.* 31 (2010) E41 author reply E42.
- [9] D. Kocur, N. Przybylko, P. Bazowski, J. Baron, Rupture during coiling of intracranial aneurysms: predictors and clinical outcome, *Clin. Neurol. Neurosurg.* 165 (2018) 81–87.
- [10] J.B. Lamano, G.G. Bushnell, H. Chen, A. Badrinathan, N.E. El Tecle, B.R. Bendok, et al., Force characterization of intracranial endovascular embolization: coil type, microcatheter placement, and insertion rate, *Neurosurgery* 75 (2014) 707–715.
- [11] N. Matsubara, S. Miyachi, Y. Nagano, T. Ohshima, O. Hososhima, T. Izumi, et al., A novel pressure sensor with an optical system for coil embolization of intracranial aneurysms, *Laboratory Invest.* 111 (2009) 41–47.
- [12] Y.K. Park, H.J. Yi, K.S. Choi, Y.J. Lee, H.J. Chun, Intraprocedural rupture during endovascular treatment of intracranial aneurysm: clinical results and literature review, *World Neurosurg.* 114 (2018) e605–e615.
- [13] A. Shamloo, M.A. Nejad, M. Saeedi, Fluid-structure interaction simulation of a cerebral aneurysm: effects of endovascular coiling treatment and aneurysm wall thickening, *J. Mech. Behav. Biomed. Mater.* 74 (2017) 72–83.
- [14] M.J. Slob, W.J. van Rooij, M. Sluzewski, Coil thickness and packing of cerebral aneurysms: a comparative study of two types of coils, *Am. J. Neuroradiol.* 26 (2005) 901–903.
- [15] M. Sluzewski, J.A. Bosch, W.J. van Rooij, P.C. Nijssen, D. Wijnalda, Rupture of intracranial aneurysms during treatment with Guglielmi detachable coils: incidence, outcome, and risk factors, *J. Neurosurg.* 94 (2001) 238–240.
- [16] J.B. White, C.G. Ken, H.J. Cloft, D.F. Kallmes, Coils in a nutshell: a review of coil physical properties, *Am. J. Neuroradiol.* 29 (2008) 1242–1246.